

## Research Article

# Interference Mitigation in Cooperative SFBC-OFDM

**D. Sreedhar and A. Chockalingam**

*Department of Electrical Communication Engineering, Indian Institute of Science, Bangalore 560012, India*

Correspondence should be addressed to A. Chockalingam, [achockal@ece.iisc.ernet.in](mailto:achockal@ece.iisc.ernet.in)

Received 15 November 2007; Accepted 28 March 2008

Recommended by Andrea Conti

We consider cooperative space-frequency block-coded OFDM (SFBC-OFDM) networks with amplify-and-forward (AF) and decode-and-forward (DF) protocols at the relays. In cooperative SFBC-OFDM networks that employ DF protocol, (i), intersymbol interference (ISI) occurs at the destination due to violation of the “quasistatic” assumption because of the frequency selectivity of the relay-to-destination channels, and (ii) intercarrier interference (ICI) occurs due to imperfect carrier synchronization between the relay nodes and the destination, both of which result in error-floors in the bit-error performance at the destination. We propose an interference cancellation algorithm for this system at the destination node, and show that the proposed algorithm effectively mitigates the ISI and ICI effects. In the case of AF protocol in cooperative networks (without SFBC-OFDM), in an earlier work, we have shown that full diversity can be achieved at the destination if phase compensation is carried out at the relays. In cooperative networks using SFBC-OFDM, however, this full-diversity attribute of the phase-compensated AF protocol is lost due to frequency selectivity and imperfect carrier synchronization on the relay-to-destination channels. We propose an interference cancellation algorithm at the destination which alleviates this loss in performance.

Copyright © 2008 D. Sreedhar and A. Chockalingam. This is an open access article distributed under the Creative Commons Attribution License, which permits unrestricted use, distribution, and reproduction in any medium, provided the original work is properly cited.

## 1. INTRODUCTION

Cooperative communications have become popular in recent research, owing to the potential for several benefits when communicating nodes in wireless networks are allowed to cooperate [1]. A classical benefit that arises from cooperation among nodes is the possibility of achieving spatial diversity, even when the nodes have only one antenna. That is, cooperation allows single-antenna nodes in a multiuser environment to share their antennas with other nodes in a distributed manner so that a given node can realize a virtual multiantenna transmitter that provides transmit diversity benefits. Such techniques, termed as “cooperative diversity” techniques, have widely been researched [2, 3]. Achieving cooperative diversity benefits based on a relay node merely repeating the information sent by a source node comes at the price of loss of throughput because the relay-to-destination transmission requires a separate time slot [3]. This loss in throughput due to repetition-based cooperation can be alleviated by integrating channel coding with cooperation [4]. Also, cooperation methods using distributed space-time coding are widely being researched [5, 6].

Recent investigations on cooperative communications focus on space-time cooperative systems based on OFDM [7–11]. Since space-time codes were developed originally for frequency-flat channels, an effective way to use them on frequency selective channels is to use them along with OFDM. A major advantage of space-time OFDM (ST-OFDM) is that a frequency selective channel is converted into multiple frequency flat channels [12], and with a proper outer code applied along with ST-OFDM code as an inner code, the full diversity of a frequency selective channel (i.e., multipath diversity) can be exploited as well. In addition to multipath diversity, user-cooperation diversity can be achieved in cooperative ST-OFDM (CO-ST-OFDM) systems, where space-time block codes (STBC) can be used in the relaying phase of cooperation [7, 8]. Accurate time and frequency synchronization, however, are crucial in achieving the promised potential of CO-ST-OFDM [8–11]. For example, in the context of cooperative OFDM, the relays-to-destination transmissions during the relaying phase of the protocol resemble transmissions from multiple noncooperating users in an uplink OFDMA system [13, 14]. Hence nonzero carrier frequency offsets (CFOs) arising due

to imperfect carrier synchronization between the relays and the destination results in multiuser interference (multiple relays viewed as virtual multiple users) at the destination. A similar effect will occur if the timing synchronization is imperfect, that is, with nonzero timing offset. Without any effort to handle this interference, the performance of cooperative OFDM may end up being worse than that of OFDM without cooperation, particularly when the synchronization errors (in terms of CFOs and timing offsets) are large, and hence interference cancellation (IC) techniques employed at the destination will be of interest. Equalization techniques to alleviate the effect of carrier frequency offsets in distributed STBC-OFDM have been reported in the literature [10]. Practical timing and frequency synchronization algorithms and channel estimation for CO-ST-OFDM using Alamouti code [15] have been investigated in [8].

An alternate way to employ space-time codes in MIMO OFDM is to perform coding across space and frequency (instead of coding across space and time), which is often referred to as space-frequency coding (SFC) [16–19]. One way to do space-frequency coding is to take space-time codes and apply them in frequency dimension instead of time dimension [16]. The advantages of using space-frequency codes along with OFDM are low delays and robustness to time-selectivity of the channel [19]. Our focus, accordingly, in this paper is on cooperative OFDM systems when space-frequency block codes (SFBC) are employed; we refer to these systems as cooperative SFBC-OFDM (CO-SFBC-OFDM) systems.

Our new contribution in this paper can be highlighted as follows. In CO-SFBC-OFDM networks that employ decode-and-forward (DF) protocol, (i) intersymbol interference (ISI) occurs at the destination due to violation of the “quasistatic” assumption because of the frequency selectivity of the relay-to-destination channels, and (ii) intercarrier interference (ICI) occurs due to imperfect carrier synchronization between the relay nodes and the destination, both of which result in error floors in the bit error performance at the destination. We propose an interference cancellation algorithm for this system at the destination node, and show that the proposed algorithm effectively mitigates the ISI and ICI effects. In the case of amplify-and-forward (AF) protocol in cooperative networks (without SFBC-OFDM), in our earlier work in [20], we have shown that full diversity can be achieved at the destination if phase compensation is carried out at the relays. In cooperative networks using SFBC-OFDM, however, this full-diversity attribute of the phase-compensated AF protocol is lost due to frequency selectivity and imperfect carrier synchronization on the relay-to-destination channels. To address this problem, we propose an interference cancellation algorithm at the destination which alleviates this loss in performance.

The rest of this paper is organized as follows. In Section 2, we present the CO-SFBC-OFDM system model with AF protocol and phase compensation at the relays, and illustrate the ISI and ICI effects. The proposed IC algorithm for this system is presented in Section 2.2. Section 3 presents the

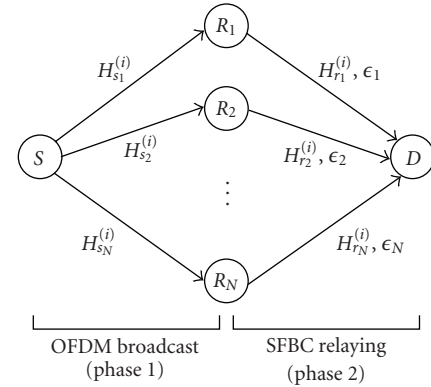


FIGURE 1: A cooperative SFBC-OFDM network consisting of one source, one destination, and  $N$  relays.

system model for CO-SFBC-OFDM system with DF protocol at the relays, and illustrates the associated ISI and ICI effects. The proposed IC algorithm for this DF protocol system is presented in Section 3.2. Results and discussions for both AF and DF protocols are presented in Section 4. Conclusions are given in Section 5.

## 2. COOPERATIVE SFBC-OFDM WITH AF PROTOCOL

Consider a wireless network as depicted in Figure 1 with  $N+2$  nodes consisting of a source, a destination and  $N$  relays. All nodes are half duplex nodes, that is, a node can either transmit or receive at a time. OFDM is used for transmission on the source-to-relays and relays-to-destination links. The destination is assumed to know (i) source-to-relays channel state information (CSI) and (ii) relays-to-destination CSI. Each relay is assumed to know the phase information of the channel from the source to itself. We employ amplification and channel phase compensation on the received signals at the relays. The transmission protocol is as follows (see Figures 1 and 2):

- (i) In the first time slot (i.e., phase 1), the source transmits information symbols  $X^{(k)}$ ,  $1 \leq k \leq M$  using an  $M$  subcarrier OFDM symbol. All the  $N$  relays receive this OFDM symbol. This phase is called the *OFDM broadcast phase*.
- (ii) In the second time slot (i.e., phase 2),  $N$  relays forward the received information. (We assume that all the relays participate in the cooperative transmission. It is also possible that some relays do not participate in the transmission based on whether the channel state is in outage or not. We do not consider such a partial participation scenario here.) For the AF protocol, the relays perform channel phase compensation and amplification on the received signal, followed by space-frequency block coding. This phase is called *AF-SFBC relay phase*. The destination receives these transmissions, performs ICI/ISI cancellation and SFBC decoding.

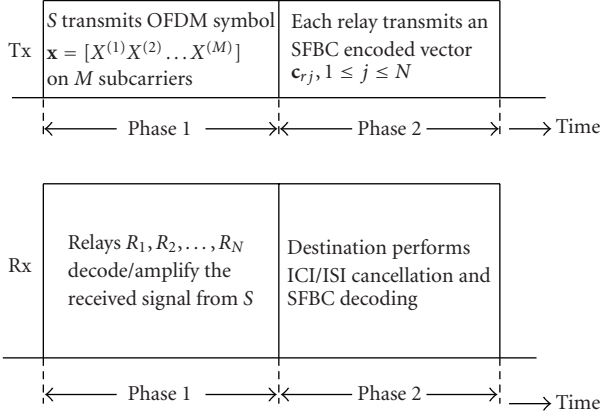


FIGURE 2: AF/DF transmission protocol in a cooperative SFBC-OFDM network.

### Broadcast reception at the relays

Let  $\mathbf{x} = [X^{(1)}, X^{(2)}, \dots, X^{(M)}]$  denote the information symbol vector transmitted by the source on  $M$  subcarriers. (We use the following notation in this paper: Bold letter uppercase is used to represent matrices and bold letter lower case is used to represent vectors.  $\Re(\cdot)$  denotes real value of a complex argument and  $\Im(\cdot)$  denotes imaginary value.  $x^{(I)}$  and  $x^{(Q)}$  denote the real and imaginary parts of the complex number  $x$ .  $(\cdot)^H$  and  $(\cdot)^T$  denote matrix conjugate transposition and matrix transposition, respectively.  $(\cdot)^*$  denotes matrix conjugation.  $\text{diag}\{a_1, a_2, \dots, a_N\}$  is a diagonal matrix having diagonal entries  $a_1, a_2, \dots, a_N$ .  $\mathbf{j}$  denotes  $\sqrt{-1}$ .  $E\{\cdot\}$  denotes expectation operation.) The received signal,  $v_{rj}^{(k)}$ , on the  $k$ th subcarrier at the  $j$ th relay during the OFDM broadcast phase can be written as

$$v_{rj}^{(k)} = \sqrt{E_1} H_{sj}^{(k)} X^{(k)} + Z_{rj}^{(k)}, \quad 1 \leq i \leq M, \quad 1 \leq j \leq N, \quad (1)$$

where  $H_{sj}^{(k)}$  is the frequency response on the  $k$ th subcarrier of the channel from source to  $j$ th relay, given by  $H_{sj}^{(k)} = \text{DFT}_M(h_{sj}^{(n)})$ , where  $h_{sj}^{(n)}$  is the time-domain impulse response of the channel from source to  $j$ th relay. (In all the source-to-relay and relay-to-destination links, we assume frequency-selective block fading channel model [21, 22]. The maximum delay spread of the channel is assumed to be less than the added guard interval. The channel is assumed to be static for one OFDM symbol duration.)  $Z_{rj}^{(k)}$  is additive white Gaussian noise with zero mean and variance  $\sigma^2$ , and  $E\{|X^{(k)}|^2\} = 1$ .  $E_1$  is the energy per symbol spent in the broadcast phase. On the source-to-relay links, all the relays listen to the source and each relay can compensate for its CFO individually. Hence there is no ISI/ICI on the source-to-relay links.

### Space-frequency block coding at the relay in AF protocol

At the relay  $j$ , first, phase compensation followed by an amplification of the received signal is done. Let  $H_{sj}^{(k)} = |H_{sj}^{(k)}| e^{j\theta_{sj}^{(k)}}$ . The operation at the relay can then be described

as (i) phase compensation (i.e, multiplication by  $e^{-j\theta_{sj}^{(k)}}$ ), and (ii) amplification on  $v_{rj}^{(k)}$  such that energy per transmission is  $E_2$ , that is,

$$\hat{v}_{rj}^{(k)} = \sqrt{\frac{E_2}{E_1 + \sigma^2}} e^{-j\theta_{sj}^{(k)}} v_{rj}^{(k)}, \quad (2)$$

$$= \sqrt{\frac{E_1 E_2}{E_1 + \sigma^2}} |H_{sj}^{(k)}| X^{(k)} + \hat{Z}_{rj}^{(k)}, \quad (3)$$

where

$$\hat{Z}_{rj}^{(k)} = \sqrt{\frac{E_2}{E_1 + \sigma^2}} e^{-j\theta_{sj}^{(k)}} Z_{rj}^{(k)}. \quad (4)$$

The space-frequency block encoding at the relays is illustrated in Figure 3. An  $N \times K$  space-time block code (STBC) matrix with  $P$  information symbols is used across subcarriers in  $N$ -relays. For the AF-SFBC relay phase transmission, we divide the  $M$  subcarriers into  $M_g$  groups such that  $M = M_g K + \kappa$ . If  $M$  is not a multiple of  $K$  then, there will not be any transmission on  $\kappa$  subcarriers, and accordingly the source will transmit only  $M_g P$  information symbols and there will be no transmission on  $M - M_g P$  subcarriers from the source. Note that  $M_g P \leq M$  since  $P/K \leq 1$  for the STBC codes considered. Now, for each relay  $j$ , we form  $M_g$  groups out of the  $M_g P$  values in  $\hat{v}_{rj}^{(k)}$ , and, for each group  $q$ , we form the  $2P \times 1$  vector  $\hat{\mathbf{v}}_{rj}^{(q)}$ , given by

$$\hat{\mathbf{v}}_{rj}^{(q)} = \left[ \hat{v}_{rj}^{((q-1)P+1)(I)}, \hat{v}_{rj}^{((q-1)P+1)(Q)}, \hat{v}_{rj}^{((q-1)P+2)(I)}, \hat{v}_{rj}^{((q-1)P+2)(Q)}, \dots, \hat{v}_{rj}^{(qP)(I)}, \hat{v}_{rj}^{(qP)(Q)} \right]^T. \quad (5)$$

The space-frequency coded symbols for the  $q$ th group of the  $j$ th relay can be obtained as

$$\begin{aligned} \mathbf{c}_{rj}^{(q)} &= \mathbf{A}_j \hat{\mathbf{v}}_{rj}^{(q)} \\ &= \sqrt{\frac{E_1 E_2}{E_1 + \sigma^2}} \mathbf{A}_j \mathbf{H}_{sj}^{(q)} \mathbf{x}^{(q)} + \mathbf{A}_j \hat{\mathbf{z}}_{rj}^{(q)}, \quad 1 \leq q \leq M_g, \end{aligned} \quad (6)$$

where the  $2P \times 2P$  matrix  $\mathbf{H}_{sj}^{(q)} = \text{diag}\{|H_{sj}^{((q-1)P+1)}|, |H_{sj}^{((q-1)P+1)}|, \dots, |H_{sj}^{(qP)}|, |H_{sj}^{(qP)}|\}$ , the  $2P \times 1$  vector  $\hat{\mathbf{z}}_{rj}^{(q)} = [\hat{Z}_{rj}^{((q-1)P+1)(I)}, \hat{Z}_{rj}^{((q-1)P+1)(Q)}, \dots, \hat{Z}_{rj}^{(qP)(I)}, \hat{Z}_{rj}^{(qP)(Q)}]^T$ , and the  $2P \times 1$  vector  $\mathbf{x}^{(q)} = [X^{((q-1)P+1)(I)}, X^{((q-1)P+1)(Q)}, \dots, X^{(qP)(I)}, X^{(qP)(Q)}]^T$ . The  $\mathbf{A}_j$  matrices perform the space-frequency encoding. For example, for the 2-relay case (i.e.,  $N = 2$ ) using Alamouti code:

$$\mathbf{A}_1 = \begin{bmatrix} 1 & 0 & \mathbf{j} & 0 \\ 0 & -1 & 0 & \mathbf{j} \end{bmatrix}, \quad \mathbf{A}_2 = \begin{bmatrix} 0 & 1 & 0 & \mathbf{j} \\ 1 & 0 & \mathbf{j} & 0 \end{bmatrix}. \quad (7)$$

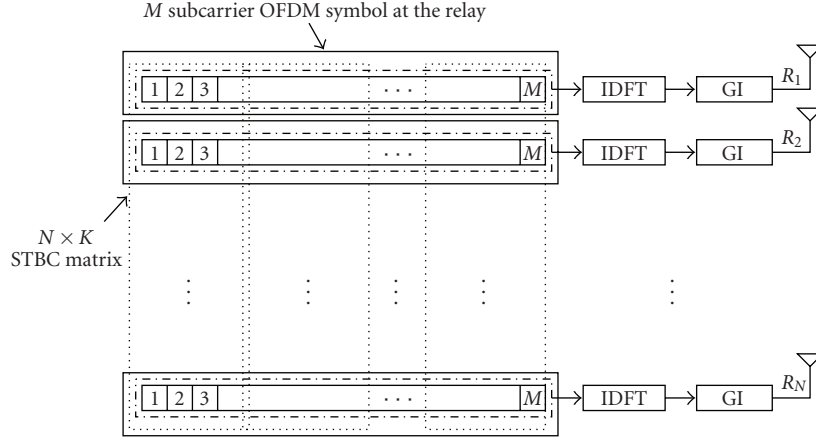


FIGURE 3: Space-frequency block coding at the relays.

The overall space-frequency coded symbol vector from the  $j$ th relay can be written as

$$\mathbf{c}_{rj} = \begin{bmatrix} \mathbf{c}_{rj}^{(1)} \\ \vdots \\ \mathbf{c}_{rj}^{(M_g)} \\ \mathbf{0}^{K \times 1} \end{bmatrix}. \quad (8)$$

Finally, the inverse Fourier transform of  $\mathbf{c}_{rj}$ , that is,  $\mathbf{t}_{rj} = \text{IDFT}(\mathbf{c}_{rj})$  is transmitted by the  $j$ th relay.

#### Received signal at the destination

The received time-domain baseband signal at the destination, after coarse carrier frequency synchronization and guard time removal, is given by

$$y^{(n)} = \sum_{j=1}^N (t_{rj}^{(n)} \star h_{jd}^{(n)}) e^{j2\pi\epsilon_j n/N} + z_d^{(n)}, \quad 0 \leq n \leq M-1, \quad (9)$$

where  $\star$  denotes linear convolution,  $h_{jd}^n$  is the channel impulse response from the  $j$ th relay to the destination. It is assumed that  $h_{jd}^n$  is nonzero only for  $n = 0, \dots, L-1$ , where  $L$  is the maximum channel delay spread. It is also assumed that the added guard interval is greater than  $L$ .  $\epsilon_j$ ,  $j = 1, \dots, N$ ,  $0 \leq |\epsilon_j| \leq 0.5$ , denotes residual carrier frequency offset (CFO) from the  $j$ th relay normalized by the subcarrier spacing, and  $z_d^{(n)}$  is the AWGN with zero mean and variance  $\sigma_d^2$ . We assume that all the nodes are time synchronized and that  $\epsilon_j$ ,  $j = 1, \dots, N$  are known at the destination. At the destination,  $y^{(n)}$  is first fed to the DFT block. The  $M \times 1$  DFT output vector,  $\mathbf{y}$ , can be written in the form

$$\mathbf{y} = \sum_{j=1}^N \mathbf{\Psi}_j \mathbf{H}_{jd} \mathbf{c}_{rj} + \mathbf{z}_d, \quad (10)$$

where  $\mathbf{\Psi}_j$  is a  $M \times M$  circulant matrix given by

$$\mathbf{\Psi}_j = \begin{bmatrix} \psi_j^{(0)} & \psi_j^{(1)} & \dots & \psi_j^{(M-1)} \\ \psi_j^{(M-1)} & \psi_j^{(0)} & \dots & \psi_j^{(M-2)} \\ \vdots & \vdots & \ddots & \vdots \\ \psi_j^{(1)} & \psi_j^{(2)} & \dots & \psi_j^{(0)} \end{bmatrix}, \quad (11)$$

where

$$\psi_j^{(k)} = \text{DFT}_M(e^{j2\pi n \epsilon_j / M}). \quad (12)$$

$\mathbf{H}_{jd}$  is the  $M \times M$  diagonal channel matrix given by  $\mathbf{H}_{jd} = \text{diag}[H_{jd}^{(1)}, H_{jd}^{(2)}, \dots, H_{jd}^{(M)}]$ , and the channel coefficient in frequency domain  $H_{jd}^{(k)}$  is given by  $H_{jd}^{(k)} = \text{DFT}_M(h_{jd}^{(n)})$ . Similarly,  $\mathbf{z}_d = [Z_d^{(1)}, Z_d^{(2)}, \dots, Z_d^{(M)}]$ , where  $Z_d^{(k)} = \text{DFT}_M(z_d^{(n)})$ . Equation (10) can be rewritten as

$$\mathbf{y} = \sum_{j=1}^N \psi_j^{(0)} \mathbf{H}_{jd} \mathbf{c}_{rj} + \underbrace{\sum_{j=1}^N (\mathbf{\Psi}_j - \psi_j^{(0)} \mathbf{I}) \mathbf{H}_{jd} \mathbf{c}_{rj}}_{\text{ICI}} + \mathbf{z}_d. \quad (13)$$

If we collect the  $K$  entries of  $\mathbf{y}$  corresponding to the  $q$ th SFBC block and form a  $K \times 1$  vector  $\mathbf{y}^{(q)}$ , then we can write

$$\mathbf{y}^{(q)} = \sum_{j=1}^N \psi_j^{(0)} \mathbf{H}_{jd}^{(q)} \mathbf{c}_{rj}^{(q)} + \sum_{j=1}^N (\mathbf{\Psi}_j - \psi_j^{(0)} \mathbf{I})^{[q]} \mathbf{H}_{jd} \mathbf{c}_{rj} + \mathbf{z}_d^{(q)}, \quad (14)$$

where  $\mathbf{H}_{jd}^{(q)} = \text{diag}[H_{jd}^{((q-1)K+1)}, \dots, H_{jd}^{(qK)}]$ ,  $\mathbf{z}_d^{(q)} = [Z_d^{((q-1)K+1)}, \dots, Z_d^{(qK)}]^T$  and  $(\cdot)^{[q]}$  denotes picking the  $K$  rows of a matrix starting from  $(q-1)K+1$ .

### Optimal ML detector and zero-forcing detector

Using (6), the  $\mathbf{c}_{rj}$  vector in (8) can be written as

$$\mathbf{c}_{rj} = \sqrt{\frac{E_1 E_2}{E_1 + \sigma^2}} \underbrace{\begin{bmatrix} \mathbf{A}_j \mathbf{H}_{sj}^{(1)} & \mathbf{0} & \cdots & \mathbf{0} & \mathbf{0} \\ \mathbf{0} & \mathbf{A}_j \mathbf{H}_{sj}^{(2)} & \cdots & \mathbf{0} & \mathbf{0} \\ \vdots & \mathbf{0} & \ddots & \vdots & \vdots \\ \mathbf{0} & \mathbf{0} & \cdots & \mathbf{A}_j \mathbf{H}_{sj}^{(M_g)} & \mathbf{0} \\ \mathbf{0} & \mathbf{0} & \cdots & \mathbf{0} & \mathbf{0} \end{bmatrix}}_{\Omega_j} \underbrace{\begin{bmatrix} \mathbf{x}^{(1)} \\ \mathbf{x}^{(2)} \\ \vdots \\ \mathbf{x}^{(M_g)} \\ \mathbf{0} \end{bmatrix}}_{\mathbf{x}} + \underbrace{\begin{bmatrix} \mathbf{A}_j \hat{\mathbf{z}}_{rj}^{(1)} \\ \mathbf{A}_j \hat{\mathbf{z}}_{rj}^{(2)} \\ \vdots \\ \mathbf{A}_j \hat{\mathbf{z}}_{rj}^{(M_g)} \\ \mathbf{0} \end{bmatrix}}_{\boldsymbol{\eta}_j}. \quad (15)$$

Substituting this in (10), we get

$$\mathbf{y} = \underbrace{\left( \sum_{j=1}^N \boldsymbol{\Psi}_j \mathbf{H}_{jd} \Omega_j \right)}_{\Phi} \mathbf{x} + \sum_{j=1}^N \boldsymbol{\Psi}_j \mathbf{H}_{jd} \boldsymbol{\eta}_j + \mathbf{z}_d. \quad (16)$$

The optimal ML detection of  $\mathbf{x}$  is given by

$$\hat{\mathbf{x}} = \arg \min_{\mathbf{x}} (\mathbf{y} - \Phi \mathbf{x})^{\mathcal{H}} \boldsymbol{\Sigma}^{-1} (\mathbf{y} - \Phi \mathbf{x}), \quad (17)$$

where  $\boldsymbol{\Sigma}$  is the covariance matrix of  $\sum_{j=1}^N \boldsymbol{\Psi}_j \mathbf{H}_{jd} \boldsymbol{\eta}_j + \mathbf{z}_d$ . This has complexity of the order  $O(\mathcal{M}^{\lfloor M/K \rfloor P})$ , where  $\mathcal{M}$  is the cardinality of the signal set used. A suboptimal zero-forcing detection can be carried out using

$$\tilde{\mathbf{y}} = (\Phi^{\mathcal{H}} \Phi)^{-1} \Phi^{\mathcal{H}} \mathbf{y}. \quad (18)$$

Since  $\Phi$  is of size  $M \times M$ , the inversion operation is of complexity  $O(M^4)$ . Interference cancellers at much lesser complexity can be adopted for the detection. In the following, we formulate the proposed ISI-ICI cancellation approach.

### Detection in frequency-flat channel in the absence of CFO

For a frequency-flat channel, all the diagonal entries of  $\mathbf{H}_{sj}^{(q)}$  and  $\mathbf{H}_{jd}^{(q)}$  become equal. Hence in frequency-flat channel with no CFO, (14) reduces to

$$\mathbf{y}^{(q)} = \sum_{j=1}^N \left| H_{sj}^{((q-1)2P+1)} \right| \left| H_{jd}^{((q-1)K+1)} \right| \mathbf{A}_j \mathbf{x}^{(q)} + \sum_{j=1}^N \mathbf{A}_j \hat{\mathbf{z}}_{rj}^{(q)} + \mathbf{z}_d^{(q)}. \quad (19)$$

Define  $\mathbf{H}_{\text{eq}}^{(q)} = \sum_{j=1}^N |H_{sj}^{((q-1)2P+1)}| |H_{jd}^{((q-1)K+1)}| \mathbf{A}_j$ . It can then be verified from the results in [20] that  $\Re(\mathbf{H}_{\text{eq}}^{(q)\mathcal{H}} \mathbf{H}_{\text{eq}}^{(q)})$  is a block diagonal matrix, and hence with the operation  $\Re(\mathbf{H}_{\text{eq}}^{(q)\mathcal{H}} \mathbf{y}^{(q)})$  it is possible to do full-diversity symbol-by-symbol detection of  $\mathbf{y}^{(q)}$ . But when the channel is frequency-selective and CFOs are nonzero, this detection gives rise to ISI and ICI, which we will analyze in the following Section 2.1.

### 2.1. ICI and ISI in AF protocol

Now we analyze the ICI and ISI at the output of the detection scheme described in Section 2, when the relays-to-destination channels as well as the source-to-relays channels are frequency-selective and when CFOs are not equal to zero. Define

$$\mathbf{H}_{\text{eq-af}}^{(q)} = \sum_{j=1}^N \sqrt{\frac{E_1 E_2}{E_1 + \sigma^2}} \psi_j^{(0)} \left| H_{sj}^{((q-1)2P+1)} \right| \left| H_{jd}^{((q-1)K+1)} \right| \mathbf{A}_j. \quad (20)$$

Since  $\sqrt{E_1 E_2 / (E_1 + \sigma^2)} \psi_j^{(0)}$  is a scalar, it is easily verified from the results in [20] that  $\Re(\mathbf{H}_{\text{eq-af}}^{(q)\mathcal{H}} \mathbf{H}_{\text{eq-af}}^{(q)})$  is a block diagonal matrix. Next, we split the channel matrices  $\mathbf{H}_{sj}^{(q)}$  and  $\mathbf{H}_{jd}^{(q)}$  into a quasistatic part and a nonquasistatic part, as

$$\mathbf{H}_{sj}^{(q)} = \underbrace{\left| H_{sj}^{((q-1)2P+1)} \right| \mathbf{I}}_{\mathbf{H}_{sj,qs}^{(q)}} + \begin{bmatrix} 0 & 0 & \cdots & 0 \\ 0 & V & \cdots & 0 \\ \vdots & \vdots & \ddots & \vdots \\ 0 & 0 & \cdots & \left| H_{sj}^{(q2P)} \right| - \left| H_{sj}^{((q-1)2P+1)} \right| \end{bmatrix}, \quad (21)$$

$$\mathbf{H}_{jd}^{(q)} = \underbrace{\left| H_{jd}^{((q-1)K+1)} \right| \mathbf{I}}_{\mathbf{H}_{jd,qs}^{(q)}} + \begin{bmatrix} 0 & 0 & \cdots & 0 \\ 0 & S & \cdots & 0 \\ \vdots & \vdots & \ddots & \vdots \\ 0 & 0 & \cdots & \left| H_{jd}^{(qK)} \right| - \left| H_{jd}^{((q-1)K+1)} \right| \end{bmatrix},$$

where  $V$  denotes  $\left| H_{sj}^{((q-1)2P+2)} \right| - \left| H_{sj}^{((q-1)2P+1)} \right|$ , and  $S$  denotes  $\left| H_{jd}^{((q-1)K+2)} \right| - \left| H_{jd}^{((q-1)K+1)} \right|$ .

Using this, the output of the operation  $\Re(\mathbf{H}_{\text{eq-af}}^{(q)\mathcal{H}} \mathbf{y}^{(q)})$  on (14) can be written as

$$\begin{aligned} \hat{\mathbf{y}}^{(q)} = & \underbrace{\Re(\mathbf{H}_{\text{eq-af}}^{(q)\mathcal{H}} \mathbf{H}_{\text{eq-af}}^{(q)}) \mathbf{x}^{(q)}}_{\text{Signal part}} \\ & + \underbrace{\Re(\mathbf{H}_{\text{eq-af}}^{(q)\mathcal{H}} \sum_{j=1}^N \psi_j^{(0)} W) \mathbf{x}^{(q)}}_{\text{ISI due to frequency-selectivity of broadcast and relay channels}} \\ & + \underbrace{\Re(\mathbf{H}_{\text{eq-af}}^{(q)\mathcal{H}} \sum_{j=1}^N (\Psi_j - \psi_j^{(0)} \mathbf{I})^{[q]} \mathbf{H}_{jd} \mathbf{c}_{rj})}_{\text{ICI due to CFOs}} \\ & + \underbrace{\Re(\mathbf{H}_{\text{eq-af}}^{(q)\mathcal{H}} (\sum_{j=1}^N \mathbf{A}_j \hat{\mathbf{z}}_{rj}^{(q)} + \mathbf{z}_d^{(q)}))}_{\text{Total noise}}, \end{aligned} \quad (22)$$

where  $W$  denotes that  $(\mathbf{H}_{jd,\text{nqs}}^{(q)} \mathbf{A}_j \mathbf{H}_{sj,\text{qs}}^{(q)} + \mathbf{H}_{jd,\text{qs}}^{(q)} \mathbf{A}_j \mathbf{H}_{sj,\text{nqs}}^{(q)} + \mathbf{H}_{jd,\text{nqs}}^{(q)} \mathbf{A}_j \mathbf{H}_{sj,\text{nqs}}^{(q)})$ .

As pointed out earlier, the optimum detector in this case would be a joint maximum-likelihood detector in  $PM_g$  variables, which has a prohibitive exponential receiver complexity.

## 2.2. Proposed ISI-ICI cancelling detector for AF protocol

In this section, we propose a two-step parallel interference canceling (PIC) receiver that cancels the frequency-selectivity-induced ISI, and the CFO-induced ICI. The proposed detector estimates and cancels the ISI (caused due to the violation of the quasistatic assumption) in the first step, and then estimates and cancels the ICI (caused due to loss of subcarrier orthogonality because of CFO) in the second step. This two-step procedure is then carried out in multiple stages. The proposed detector is presented in the following.

As can be seen, (22) identifies the desired signal, ISI, ICI, and noise components present in the output  $\hat{\mathbf{y}}^{(q)}$ . Based on this received signal model and the knowledge of the matrices  $\mathbf{H}_{jd,\text{nqs}}^{(q)}$ ,  $\mathbf{H}_{jd,\text{qs}}^{(q)}$ ,  $\mathbf{H}_{sj,\text{nqs}}^{(q)}$ ,  $\mathbf{H}_{sj,\text{qs}}^{(q)}$ , and  $\mathbf{H}_{\text{eq-af}}^{(q)}$ , for all  $q, j$  we formulate the proposed interference estimation and cancellation procedure as follows.

- (1) For each space-frequency code block  $q$ , estimate the information symbols  $\hat{\mathbf{x}}^{(q)}$  from (22), ignoring ISI and ICI.
- (2) For each space-frequency code block  $q$ , obtain an estimate of the ISI (i.e., an estimate of the ISI term in (22)) from the estimated symbols  $\hat{\mathbf{x}}^{(q)}$  in the previous step.
- (3) Cancel the estimated ISI from  $\hat{\mathbf{y}}^{(q)}$ .
- (4) Using  $\hat{\mathbf{x}}^{(q)}$  from step 1, regenerate  $\hat{\mathbf{c}}^{(q)}$  using (6). Then, using  $\hat{\mathbf{c}}^{(q)}$ , obtain an estimate of the ICI (i.e., an estimate of the ICI term in (22)).

- (5) Cancel the estimated ICI from the ISI-canceled output in step 3.
- (6) Take the ISI- and ICI-canceled output from step 5 as the input back to step 1 (for the next stage of cancellation).

Based on the above, and  $\Lambda_{\text{af}}^{(q)} = \Re(\mathbf{H}_{\text{eq-af}}^{(q)\mathcal{H}} \mathbf{H}_{\text{eq-af}}^{(q)})$ , the cancellation algorithm for the  $m$ th stage can be summarized as in Algorithm 1.

It is noted that Algorithm 1 has polynomial complexity. Also,  $\Lambda_{\text{af}}^{(q)}$  is a full-rank block diagonal matrix, and its inversion in the second equation in Algorithm 1 is simple. Assuming that the multiplication of the matrices  $\mathbf{A}_j$  with  $\mathbf{H}_{sj}$ ,  $\mathbf{H}_{jd}$  could be precomputed, the total number of complex multiplications required for  $m$  stages of the proposed iterative interference cancellation is  $2P \lfloor M/K \rfloor (K + 2P + (m - 1)(4P + 2K + NK))$ , which is much less complex than the zero-forcing detector complexity of  $O(M^4)$ .

## 3. COOPERATIVE SFBC-OFDM WITH DF PROTOCOL

The broadcast phase of the transmission protocol is the same for both AF protocol as well as DF protocol. In the relay phase of the DF protocol, however, the relays decode the information (instead of merely amplifying it) sent by the source, and transmits a space-frequency encoded version of this decoded information. This phase is called *DF-SFBC relay phase*. The destination receives this transmission, does ISI and ICI cancellation, followed by SFBC decoding.

### Space-frequency block coding at the relay in DF protocol

We employ the same space-frequency encoding strategy as in AF protocol, except that instead of an amplification operation in (2) at the relay  $j$ , a decoding of the information symbols is done, that is, the decoded symbol on the  $k$ th subcarrier at the  $j$ th relay, denoted by  $\tilde{X}_j^{(k)}$ , is obtained as

$$\tilde{X}_j^{(k)} = \sqrt{E_2} \left( \arg \min_{X^{(k)}} \left\| v_{rj}^{(k)} - \sqrt{E_1} H_{sj}^{(k)} X^{(k)} \right\|^2 \right), \quad (23)$$

$$1 \leq i \leq M_g P, \quad 1 \leq j \leq N,$$

where  $E_2$  is the energy per transmission in the relay phase. The corresponding space-frequency coded symbols for the  $q$ th group of subcarriers of the  $j$ th relay is obtained as

$$\mathbf{c}_{rj}^{(q)} = \mathbf{A}_j \tilde{\mathbf{x}}_j^{(q)}, \quad (24)$$

where  $\tilde{\mathbf{x}}_j^{(q)} = [\tilde{X}_j^{((q-1)P+1),(I)}, \tilde{X}_j^{((q-1)P+1),(Q)}, \dots, \tilde{X}_j^{(qP),(I)}, \tilde{X}_j^{(qP),(Q)}]^T$ . The received signal model at the destination in the DF protocol is the same as in (14), with  $\mathbf{c}_{rj}^{(q)}$  generated as in (24). It is possible that the symbol vector  $\mathbf{x}$  is detected differently at each relay. For the purpose of developing the IC algorithm, however, and henceforth in this paper, we assume that  $\tilde{\mathbf{x}}_j^{(q)} = \tilde{\mathbf{x}}_k^{(q)} \forall j, k$  and drop the  $j$  index from  $\tilde{\mathbf{x}}_j^{(q)}$ . In all our simulations, however, we will use the actual  $\tilde{\mathbf{x}}_j^{(q)}$ 's at the relays.

*Initialization:* Set  $m = 1$ .  
*Evaluate*

$$\hat{\mathbf{y}}^{(q,m)} = \Re(\mathbf{H}_{\text{eq-af}}^{(q)} \mathcal{H} \mathbf{y}^{(q)}), \quad 1 \leq q \leq M_g.$$

*Loop*  
*Estimate*

$$\hat{\mathbf{x}}^{(q,m)} = (\mathbf{A}_{\text{af}}^{(q)})^{-1} \hat{\mathbf{y}}^{(q,m)}, \quad 1 \leq q \leq M_g.$$

*Cancel ISI*  
 $\hat{\mathbf{y}}^{(q,m+1)} = \hat{\mathbf{y}}^{(q,1)}$

$$-\Re\left(\mathbf{H}_{\text{eq-af}}^{(q)} \mathcal{H} \sum_{j=1}^N \psi_j^{(0)} \left(\mathbf{H}_{j,d,\text{nqs}}^{(q)} \mathbf{A}_j \mathbf{H}_{s_j,\text{qs}}^{(q)} + \mathbf{H}_{j,d,\text{qs}}^{(q)} \mathbf{A}_j \mathbf{H}_{s_j,\text{nqs}}^{(q)} + \mathbf{H}_{j,d,\text{nqs}}^{(q)} \mathbf{A}_j \mathbf{H}_{s_j,\text{nqs}}^{(q)}\right)\right) \hat{\mathbf{x}}^{(q,m)},$$

$$1 \leq q \leq M_g.$$

*Form  $\hat{\mathbf{c}}_{r_j}^{(q,m)}$  from*

$$\hat{\mathbf{c}}_{r_j}^{(q,m)} = \sqrt{\frac{E_1 E_2}{E_1 + \sigma^2}} \mathbf{A}_j \mathbf{H}_{s_j}^{(q)} \hat{\mathbf{x}}^{(q,m)}, \quad 1 \leq q \leq M_g, \quad 1 \leq j \leq N.$$

*Stack  $\hat{\mathbf{c}}_{r_j}^{(q,m)}$  and form  $\hat{\mathbf{c}}_{r_j}^{(m)}$*   
*Cancel ICI*

$$\hat{\mathbf{y}}^{(q,m+1)} = \hat{\mathbf{y}}^{(q,m+1)} - \Re\left(\mathbf{H}_{\text{eq-af}}^{(q)} \mathcal{H} \sum_{j=1}^N (\mathbf{\Psi}_j - \psi_j^{(0)} \mathbf{I})^{[q]} \mathbf{H}_{j,d} \hat{\mathbf{c}}_{r_j}^{(m)}\right), \quad 1 \leq q \leq M_g.$$

$m = m + 1$  goto *Loop*.

ALGORITHM 1

### Detection in frequency-flat channel in the absence of CFO

For a frequency-flat channel (i.e.,  $\mathbf{H}_{j,d}^{(q)} = H_{j,d}^{((q-1)K+1)} \mathbf{I}$ ) with no carrier frequency offset (i.e.,  $\epsilon_j = 0 \forall j$ ), (14) reduces to

$$\mathbf{y}^{(q)} = \sum_{j=1}^N H_{j,d}^{((q-1)K+1)} \mathbf{A}_j \tilde{\mathbf{x}}^{(q)} + \mathbf{z}_d^{(q)}. \quad (25)$$

Define  $\mathbf{H}_{\text{eq}}^{(q)} = \sum_{j=1}^N H_{j,d}^{((q-1)K+1)} \mathbf{A}_j$ . Then, by the properties of  $\mathbf{A}_j$  given in [20],  $\Re(\mathbf{H}_{\text{eq}}^{(q)} \mathcal{H} \mathbf{H}_{\text{eq}}^{\prime(q)})$  is a block diagonal matrix containing  $2 \times 2$  matrices as diagonal entries. Hence it is possible to do full-diversity symbol-by-symbol detection with the operation  $\Re(\mathbf{H}_{\text{eq}}^{(q)} \mathcal{H} \mathbf{y}^{(q)})$ . As in AF protocol, when the channel is frequency-selective and CFOs are nonzero, this detection gives rise to ISI and ICI.

### 3.1. ICI and ISI in DF protocol

Now, we analyze the ICI and ISI at the output of the diversity combining operation when the relays-to-destination channels are frequency-selective and CFOs are nonzero. Define

$$\mathbf{H}_{\text{eq-df}}^{(q)} = \sum_{j=1}^N \psi_j^{(0)} H_{j,d}^{((q-1)K+1)} \mathbf{A}_j. \quad (26)$$

Since  $\psi_j^{(0)}$  is a scalar,  $\Re(\mathbf{H}_{\text{eq-df}}^{(q)} \mathcal{H} \mathbf{H}_{\text{eq-df}}^{\prime(q)})$  is also a block diagonal matrix. If  $\mathbf{H}_{j,d}^{(q)}$  matrix is split as in (21), the output of the operation  $\Re(\mathbf{H}_{\text{eq-df}}^{(q)} \mathcal{H} \mathbf{y}^{(q)})$  on (14) can be written as

$$\begin{aligned} \hat{\mathbf{y}}^{(q)} = & \underbrace{\Re(\mathbf{H}_{\text{eq-df}}^{(q)} \mathcal{H} \mathcal{H}_{\text{eq-df}}^{(q)} \tilde{\mathbf{x}}^{(q)})}_{\text{Signal part}} \\ & + \underbrace{\Re(\mathbf{H}_{\text{eq-df}}^{(q)} \mathcal{H} \sum_{j=1}^N \psi_j^{(0)} \mathbf{H}_{j,d,\text{nqs}}^{(q)} \mathbf{A}_j \tilde{\mathbf{x}}^{(q)})}_{\text{ISI}} \\ & + \underbrace{\Re(\mathbf{H}_{\text{eq-df}}^{(q)} \mathcal{H} \sum_{j=1}^N (\mathbf{\Psi}_j - \psi_j^{(0)} \mathbf{I})^{[q]} \mathbf{H}_{j,d} \mathbf{c}_{r_j})}_{\text{ICI due to CFOs}} \\ & + \underbrace{\Re(\mathbf{H}_{\text{eq-df}}^{(q)} \mathcal{H} \mathbf{z}_d^{(q)})}_{\text{Total noise}}. \end{aligned} \quad (27)$$

As in AF protocol, the optimum detector in this case would be a maximum likelihood detector in  $PM_g$  variables, which has prohibitive exponential receiver complexity.

### 3.2. Proposed ISI-ICI cancelling detector for DF protocol

Similar to the AF protocol, we propose a two-step PIC receiver for the DF protocol that cancels the frequency-selectivity induced ISI, and the CFO induced ICI. As can be seen, (27) identifies the desired signal, ISI, ICI, and noise components present in the output  $\hat{\mathbf{y}}^{(q)}$ . Based on this received signal model and the knowledge of the matrices  $\mathbf{H}_{j,d,\text{nqs}}^{(q)}$ ,  $\mathbf{H}_{j,d,\text{qs}}^{(q)}$ , and  $\mathbf{H}_{\text{eq-df}}^{(q)}$  for all  $q, j$ , we formulate the proposed interference estimation and cancellation procedure. Let  $\mathbf{A}_{\text{df}}^{(q)} = \Re(\mathbf{H}_{\text{eq-df}}^{(q)} \mathcal{H} \mathbf{H}_{\text{eq-df}}^{\prime(q)})$ . The cancellation algorithm for the  $m$ th stage can be summarized as in Algorithm 2.

*Initialization:* Set  $m = 1$ .

*Evaluate*

$$\hat{\mathbf{y}}^{(q,m)} = \Re\left(\mathbf{H}_{\text{eq-df}}^{(q)} \mathcal{H} \mathbf{y}^{(q)}\right), \quad 1 \leq q \leq M_g.$$

*Loop*

*Estimate*

$$\hat{\mathbf{x}}^{(q,m)} = (\mathbf{\Lambda}_{\text{df}}^{(q)})^{-1} \hat{\mathbf{y}}^{(q,m)}, \quad 1 \leq q \leq M_g.$$

*Cancel ISI*

$$\hat{\mathbf{y}}^{(q,m+1)} = \hat{\mathbf{y}}^{(q,1)} - \Re\left(\mathbf{H}_{\text{eq-af}}^{(q)} \sum_{j=1}^N \psi_j^{(0)} \mathbf{H}_{j\text{d,nqs}}^{(q)} \mathbf{A}_j\right) \hat{\mathbf{x}}^{(q,m)}, \quad 1 \leq q \leq M_g.$$

*Form  $\hat{\mathbf{c}}_{r_j}^{(q,m)}$  from*

$$\hat{\mathbf{c}}_{r_j}^{(q,m)} = \sqrt{E_2} \mathbf{A}_j \hat{\mathbf{x}}^{(q,m)}, \quad 1 \leq q \leq M_g, \quad 1 \leq j \leq N.$$

*Stack  $\hat{\mathbf{c}}_{r_j}^{(q,m)}$  and form  $\hat{\mathbf{c}}_{r_j}^{(m)}$*

*Cancel ICI*

$$\hat{\mathbf{y}}^{(q,m+1)} = \hat{\mathbf{y}}^{(q,m+1)} - \Re\left(\mathbf{H}_{\text{eq-df}}^{(q)} \sum_{j=1}^N (\mathbf{\Psi}_j - \psi_j^{(0)} \mathbf{I})^{[q]} \mathbf{H}_{j\text{d}} \hat{\mathbf{c}}_{r_j}^{(m)}\right), \quad 1 \leq q \leq M_g.$$

$m = m + 1$  goto *Loop*.

ALGORITHM 2

The order of complexity for Algorithm 2 is the same as that of the algorithm for AF protocol presented in Section 2.2.

#### 4. SIMULATION RESULTS AND DISCUSSIONS

##### Simulation results for AF protocol

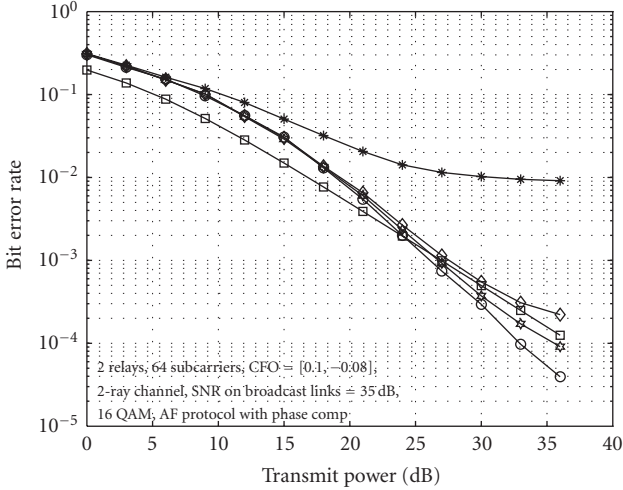
In this section, we evaluate the BER performance of the proposed interference cancelling receiver through simulations for the AF protocol in CO-SFBC-OFDM. For all the simulations, the total transmit power per symbol is equally divided between broadcast phase and relay phase. The noise variance at the destination is kept at unity and the transmit power per bit is varied. When there is no noise at the relays, then the transmit power per bit will be equal to the SNR per bit. We consider the following codes [23] in our simulations:

$$\begin{aligned}
 G_2 &= \begin{pmatrix} x_1 & x_2 \\ -x_2^* & x_1^* \end{pmatrix}, \\
 G_4 &= \begin{pmatrix} x_1 & x_2 & x_3 & 0 \\ -x_2^* & x_1^* & 0 & x_3 \\ -x_3^* & 0 & x_1 & x_2 \\ 0 & -x_3^* & -x_2^* & x_1^* \end{pmatrix}, \\
 G_8 &= \begin{pmatrix} x_1 & x_2 & x_3 & 0 & x_4 & 0 & 0 & 0 \\ -x_2^* & x_1^* & 0 & x_3 & 0 & x_4 & 0 & 0 \\ -x_3^* & 0 & x_1 & x_2 & 0 & 0 & x_4 & 0 \\ 0 & -x_3^* & -x_2^* & x_1^* & 0 & 0 & 0 & x_4 \\ -x_4^* & 0 & 0 & 0 & x_1 & x_2 & x_3 & 0 \\ 0 & -x_4^* & 0 & 0 & -x_2^* & x_1^* & 0 & x_3 \\ 0 & 0 & -x_4^* & 0 & -x_3^* & 0 & x_1 & x_2 \\ 0 & 0 & 0 & -x_4^* & 0 & -x_3^* & -x_2^* & x_1^* \end{pmatrix}.
 \end{aligned} \tag{28}$$

First, in Figure 4, we present the performance of a two-relay CO-SFBC-OFDM scheme using  $G_2$  code. The received SNRs at all the relays are set to 35 dB. Two-ray, equal-power Rayleigh fading channel model is used for all the links. Number of subcarriers used is  $M = 64$  and modulation used is 16-QAM. The CFO values at the destination for relays 1 and 2,  $[\epsilon_1, \epsilon_2]$ , are taken to be  $[0.1, -0.08]$ . We plot the BER performance of CO-SFBC-OFDM without IC and with 2 and 3 stages ( $m = 2, 3$ ) of IC. The BER performance of noncooperative OFDM (i.e., simple point-to-point OFDM) which has the same power per transmitted bit as that of CO-SFBC-OFDM is also plotted for comparison. For CO-SFBC-OFDM, we also plot the performance of an ideal case when there is no interference, that is, when CFO =  $[0, 0]$  and  $L = 1$  (frequency-flat fading). From Figure 4, it can be seen that without interference cancellation, the performance of CO-SFBC-OFDM is worse than that of noncooperative OFDM. The performance improves significantly with 2 and 3 stages of cancellation, and it approaches the ideal performance of cooperation without interference. For example, at a BER of  $10^{-2}$ , the performance improves by 12 dB with 3 stages of cancellation compared to no cancellation, and it is 0.5 dB close to the ideal performance. It can be seen that, at low SNRs, the ideal performance with cooperation is worse than that of no cooperation. This is because of the half-power split of CO-SFBC-OFDM between broadcast and relay phases. It can be observed that the slope of the BER curve of the ideal performance is steeper (2nd order diversity) than that of no cooperation (1st order diversity), and the crossover due to this diversity order difference happens at around 24 dB.

Next, in Figure 5, we repeat the same experiment (as in Figure 4) with 3 relays using  $G_3$  code, which is obtained by deleting one column from  $G_4$  code in (38–40). The CFO values at the destination for relays 1, 2, and 3,  $[\epsilon_1, \epsilon_2, \epsilon_3]$ , are taken to be  $[0.1, -0.08, 0.06]$ . Similar observations on the performance as in Figure 4 can be made in Figure 5 also.





- \*  $L = 2$ , nonzero CFO, no IC
- ◇  $L = 2$ , nonzero CFO, IC,  $m = 2$
- \*  $L = 2$ , nonzero CFO, IC,  $m = 3$
- $L = 1$ , CFO = 0, (ideal)
- Non-cooperative OFDM

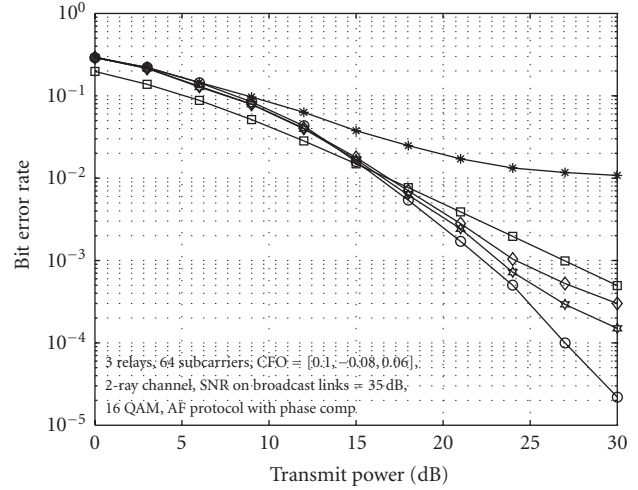
FIGURE 4: BER performance as a function of SNR for CO-SFBC-OFDM on frequency-selective fading ( $L = 2$ ).  $M = 64$ , 2 relays ( $N = 2$ ,  $G_2$  code), CFO = [0.1, -0.08], 16-QAM, SNR on broadcast links = 35 dB. AF protocol and phase compensation at the relays.

For example, at a BER of  $10^{-2}$ , the performance of CO-SFBC-OFDM improves by over 5 dB because of interference cancellation compared to no cancellation. The difference is less compared to  $G_2$  code because of higher-order diversity (3rd order diversity) in this case of  $G_3$  code.

In Figure 6, we present the effect of number of relays on the performance of the interference cancellation algorithm. Codes  $G_2, G_3, G_4$ , and  $G_8$  are used to evaluate the performance with 2, 3, 4 and 8 relays, respectively. The received SNRs at the relays are set to 45 dB. The CFOs for the different relays are [0.1, -0.08, 0.06, 0.12, -0.04, 0.02, 0.01, -0.07] and all the channels are assumed to be 2-ray, equal-power Rayleigh channels. The transmit power is kept at 18 dB per bit. The BER performance of noncooperative OFDM and no interference ( $L = 1$ , CFO = 0, ideal) are also plotted. It can be observed that without IC, the performance of CO-SFBC-OFDM is worse than no cooperation and the performance improves with increasing stages of IC and approaches the ideal performance for all the cases considered. It can also be observed that performance improves with increase in number of relays, and the returns are diminishing with increase in number of relays.

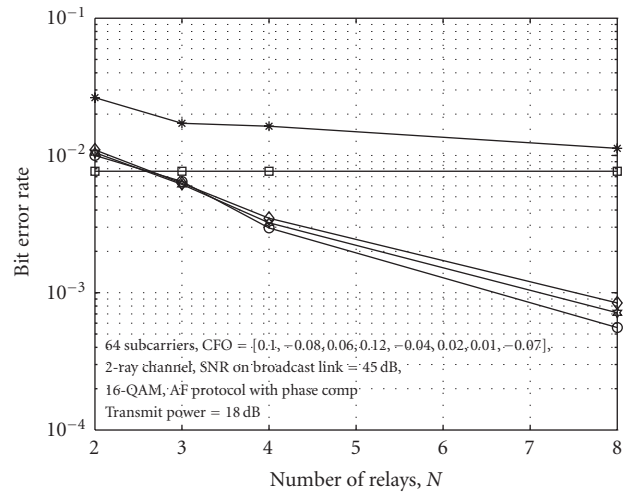
*Simulation results for DF protocol*

In Figures 7, 8, and 9, we repeat the same experiments as in Figures 4, 5, and 6, respectively, for DF protocol at the relays. For  $G_2$  code, from Figure 7, it can be observed that the performance without IC is worse than no cooperation. The performance improves with increasing number of



- \*  $L = 2$ , nonzero CFO, no IC
- ◇  $L = 2$ , nonzero CFO, IC,  $m = 2$
- \*  $L = 2$ , nonzero CFO, IC,  $m = 3$
- $L = 1$ , CFO = 0, (ideal)
- Non-cooperative OFDM

FIGURE 5: BER performance as a function of SNR for CO-SFBC-OFDM on frequency-selective fading ( $L = 2$ ).  $M = 64$ , 3 relays ( $N = 3$ ,  $G_3$  code), CFO = [0.1, -0.08, 0.06], 16-QAM, SNR on broadcast links = 35 dB. AF protocol and phase compensation at the relays.



- \*  $L = 2$ , nonzero CFO, no IC
- ◇  $L = 2$ , nonzero CFO, IC,  $m = 2$
- \*  $L = 2$ , nonzero CFO, IC,  $m = 3$
- $L = 1$ , CFO = 0, (ideal)
- Non-cooperative OFDM

FIGURE 6: BER performance as a function of number of relays for CO-SFBC-OFDM on frequency-selective fading ( $L = 2$ ).  $M = 64$ , Transmit power = 18 dB per bit. CFO = [0.1, -0.08, 0.06, 0.12, -0.04, 0.02, 0.01, -0.07], 16-QAM, SNR on broadcast links = 45 dB.  $G_2, G_3, G_4$  and  $G_8$  codes with rates 1, 3/4, 3/4 and 1/2 are used. AF protocol and phase compensation at the relays.

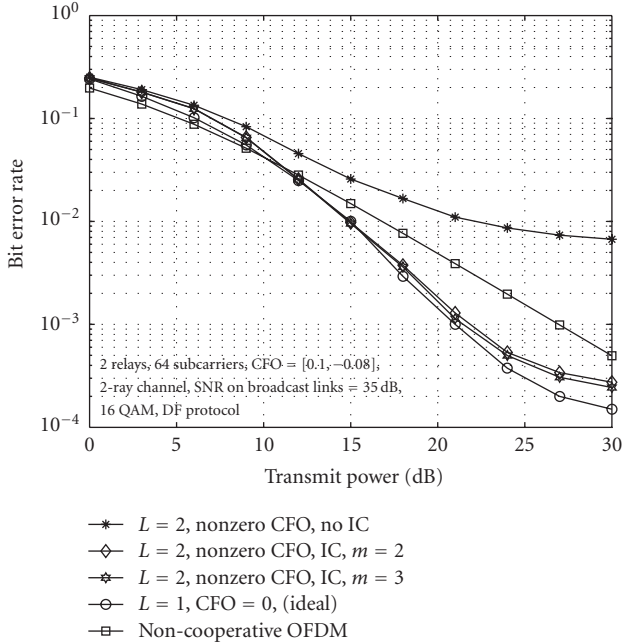


FIGURE 7: BER performance as a function of SNR for CO-SFBC-OFDM on frequency-selective fading ( $L = 2$ ).  $M = 64$ , 2 relays ( $N = 2$ ,  $G_2$  code), CFO = [0.1, -0.08], 16-QAM, SNR in broadcast links = 35 dB. DF protocol at the relays.

cancellation stages. For example, at a BER of  $10^{-2}$ , there is a 6 dB improvement with 3 stages of cancellation. It can also be observed that crossover between CO-SFBC-OFDM (ideal) and no cooperation happens at a transmit power of 12 dB. For  $G_3$  code also, Figure 8 shows similar performance improvement with IC. Figure 9 shows the performance plots for different number of relays using  $G_2$ ,  $G_3$ ,  $G_4$ , and  $G_8$  codes. Finally, comparing the performances of AF and DF protocols, that is, Figures 4 with 7, 5 with 8, and 6 with 9, it can be observed that DF protocol has better performance compared to AF protocol for all the cases considered.

## 5. CONCLUSIONS

In this paper, we addressed the issue of interference (ISI and ICI due to synchronization errors and frequency selectivity of the channel) when SFBC codes are employed in cooperative OFDM systems, and proposed a low-complexity interference mitigation approach. We proposed an interference cancellation algorithm for a CO-SFBC-OFDM system with AF protocol and phase compensation at the relays. We also proposed an interference cancellation algorithm for the same system when DF protocol is used at the relays, instead of AF protocol with phase compensation. Our simulation results showed that, with the proposed algorithms, the performance of the CO-SFBC-OFDM was better than OFDM without cooperation even in the presence of carrier synchronization errors. It is also shown that DF protocol performs better than the AF protocol in these CO-SFBC-OFDM systems. The proposed IC algorithms can be extended to handle the

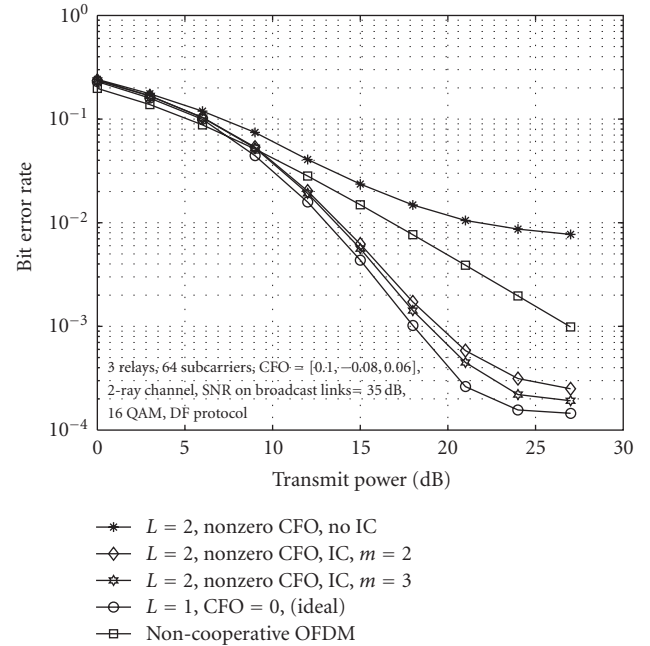


FIGURE 8: BER performance as a function of SNR for CO-SFBC-OFDM on frequency-selective fading ( $L = 2$ ).  $M = 64$ , 3 relays ( $N = 3$ ,  $G_3$  code), CFO = [0.1, -0.08, 0.06], 16-QAM, SNR in broadcast links = 35 dB. DF protocol at the relays.

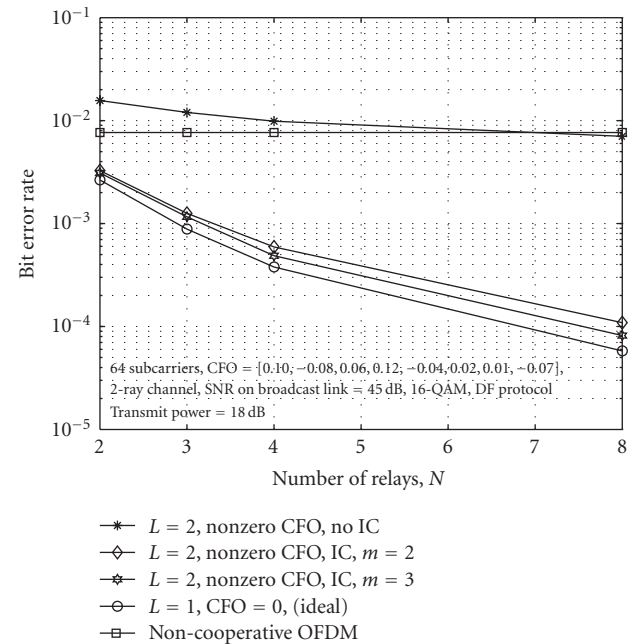


FIGURE 9: BER performance as a function of number of relays for CO-SFBC-OFDM on frequency-selective fading ( $L = 2$ ).  $M = 64$ , at a transmit power of 18 dB per bit. CFO = [0.1, -0.08, 0.06, 0.12, -0.04, 0.02, 0.01, -0.07], 16-QAM, SNR in broadcast links = 45 dB.  $G_2$ ,  $G_3$ ,  $G_4$  and  $G_8$  codes with rates 1, 3/4, 3/4 and 1/2 are used. DF protocol is employed at the relays.

ISI effects caused due to imperfect timing on the relays-to-destination channels, that is, due to nonzero timing offsets at the destination. In the simulation results presented, the receiver is assumed to know the exact channel state information. The performance is expected to deteriorate when the receiver has only an estimated channel state information. The analysis of this deterioration and possible ways of mitigating this would be an interesting area of future work. Also, it is assumed that the relays are always available for cooperation. Algorithms to “discover” the nodes that could participate in the cooperation could also be an area of future work.

## ACKNOWLEDGMENTS

This work in part was presented in the IEEE PIMRC'2007, Athens, September 2007. This work was supported in part by the Swarnajayanti Fellowship, Department of Science and Technology, New Delhi, Government of India, under Project Ref: No.6/3/2002-S.F, and the DRDO-IISc Program on Advanced Research in Mathematical Engineering.

## REFERENCES

- [1] A. Nosratinia, T. E. Hunter, and A. Hedayat, “Cooperative communication in wireless networks,” *IEEE Communications Magazine*, vol. 42, no. 10, pp. 74–80, 2004.
- [2] A. Sendonaris, E. Erkip, and B. Aazhang, “User cooperation diversity—part I: system description,” *IEEE Transactions on Communications*, vol. 51, no. 11, pp. 1927–1938, 2003.
- [3] J. N. Laneman, D. N. C. Tse, and G. W. Wornell, “Cooperative diversity in wireless networks: efficient protocols and outage behavior,” *IEEE Transactions on Information Theory*, vol. 50, no. 12, pp. 3062–3080, 2004.
- [4] T. E. Hunter and A. Nosratinia, “Diversity through coded cooperation,” *IEEE Transactions on Wireless Communications*, vol. 5, no. 2, pp. 283–289, 2006.
- [5] J. N. Laneman and G. W. Wornell, “Distributed space-time coded protocols for exploiting cooperative diversity in wireless networks,” *IEEE Transactions on Information Theory*, vol. 49, no. 10, pp. 2415–2426, 2003.
- [6] S. Yiu, R. Schober, and L. Lampe, “Distributed space-time block coding,” *IEEE Transactions on Communications*, vol. 54, no. 7, pp. 1195–1206, 2006.
- [7] L. Yu and A. Stefanov, “Cooperative space-time coding for MIMO OFDM systems,” in *Proceedings of the IEEE Military Communications Conference (MILCOM '05)*, vol. 2, pp. 990–995, Atlantic City, NJ, USA, October 2005.
- [8] O.-S. Shin, A. M. Chan, H. T. Kung, and V. Tarokh, “Design of an OFDM cooperative space-time diversity system,” *IEEE Transactions on Vehicular Technology*, vol. 56, no. 4, part 2, pp. 2203–2215, 2007.
- [9] F. Ng and X. Li, “Cooperative STBC-OFDM transmissions with imperfect synchronization in time and frequency,” in *Proceedings of the 39th Asilomar Conference on Signals, Systems and Computers*, pp. 524–528, Pacific Grove, Calif, USA, October–November 2005.
- [10] Z. Li, D. Qu, and G. Zhu, “An equalization technique for distributed STBC-OFDM system with multiple carrier frequency offsets,” in *Proceedings of the IEEE Wireless Communications and Networking Conference (WCNC '06)*, vol. 2, pp. 839–843, Las Vegas, Nev, USA, April 2006.
- [11] Y. Mei, Y. Hua, A. Swami, and B. Daneshrad, “Combating synchronization errors in cooperative relays,” in *Proceedings of the IEEE International Conference on Acoustics, Speech and Signal Processing (ICASSP '05)*, vol. 3, pp. 369–372, Philadelphia, Pa, USA, March 2005.
- [12] E. G. Larsson and P. Stoica, *Space-Time Block Coding for Wireless Communications*, Cambridge University Press, Cambridge, UK, 2003.
- [13] D. Huang and K. B. Letaief, “An interference-cancellation scheme for carrier frequency offsets correction in OFDMA systems,” *IEEE Transactions on Communications*, vol. 53, no. 7, pp. 1155–1165, 2005.
- [14] S. Manohar, D. Sreedhar, V. Tikiya, and A. Chockalingam, “Cancellation of multiuser interference due to carrier frequency offsets in uplink OFDMA,” *IEEE Transactions on Wireless Communications*, vol. 6, no. 7, pp. 2560–2571, 2007.
- [15] S. M. Alamouti, “A simple transmit diversity technique for wireless communications,” *IEEE Journal on Selected Areas in Communications*, vol. 16, no. 8, pp. 1451–1458, 1998.
- [16] H. Bölcskei and A. J. Paulraj, “Space-frequency coded broadband OFDM systems,” in *Proceedings of the IEEE Wireless Communications and Networking Conference (WCNC '00)*, vol. 1, pp. 1–6, Chicago, Ill, USA, September 2000.
- [17] Z. Liu, Y. Xin, and G. B. Giannakis, “Space-time-frequency coded OFDM over frequency-selective fading channels,” *IEEE Transactions on Signal Processing*, vol. 50, no. 10, pp. 2465–2476, 2002.
- [18] Y. Gong and K. B. Letaief, “An efficient space-frequency coded wideband OFDM system for wireless communications,” *IEEE Transactions on Communications*, vol. 51, no. 12, pp. 2019–2029, 2003.
- [19] D. Sreedhar and A. Chockalingam, “Detection of SFBC-OFDM signals in frequency- and time-selective MIMO channels,” in *Proceedings of the IEEE Wireless Communications and Networking Conference (WCNC '07)*, pp. 852–857, Kowloon, Hong Kong, March 2007.
- [20] D. Sreedhar, A. Chockalingam, and B. S. Rajan, “Single-symbol ML decodable distributed STBCs for partially-coherent cooperative networks,” submitted to *IEEE Transactions on Information Theory*.
- [21] E. Malkamäki and H. Leib, “Evaluating the performance of convolutional codes over block fading channels,” *IEEE Transactions on Information Theory*, vol. 45, no. 5, pp. 1643–1646, 1999.
- [22] M. Chiani, A. Conti, and O. Andrisano, “Outage evaluation for slow frequency-hopping mobile radio systems,” *IEEE Transactions on Communications*, vol. 47, no. 12, pp. 1865–1874, 1999.
- [23] V. Tarokh, H. Jafarkhani, and A. R. Calderbank, “Space-time block codes from orthogonal designs,” *IEEE Transactions on Information Theory*, vol. 45, no. 5, pp. 1456–1467, 1999.